

Supporting Information

Luo et al. 10.1073/pnas.1303231110

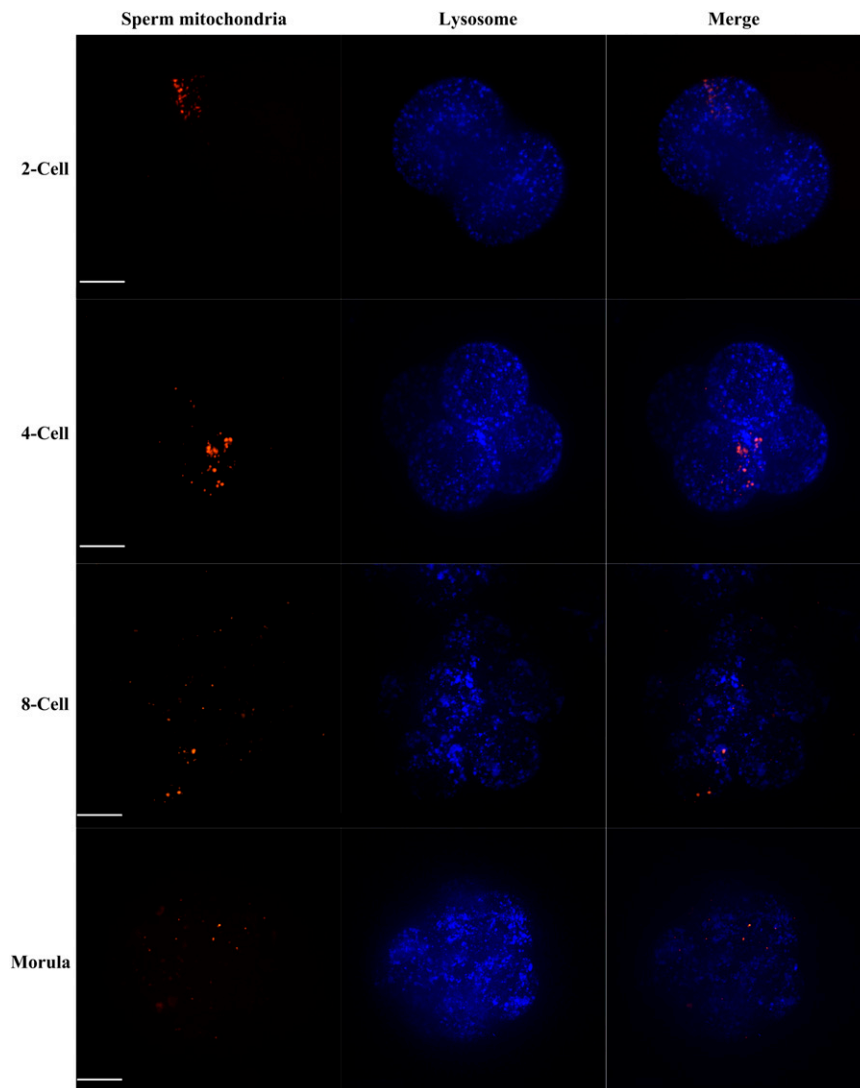


Fig. S1. Live cell fluorescence imaging of sperm mitochondria (red) and lysosomes (blue) in early embryos. No sperm mitochondria were engulfed by lysosomes before the morula stage until sperm mitochondria disappeared. (Scale bars: 20 μm .)

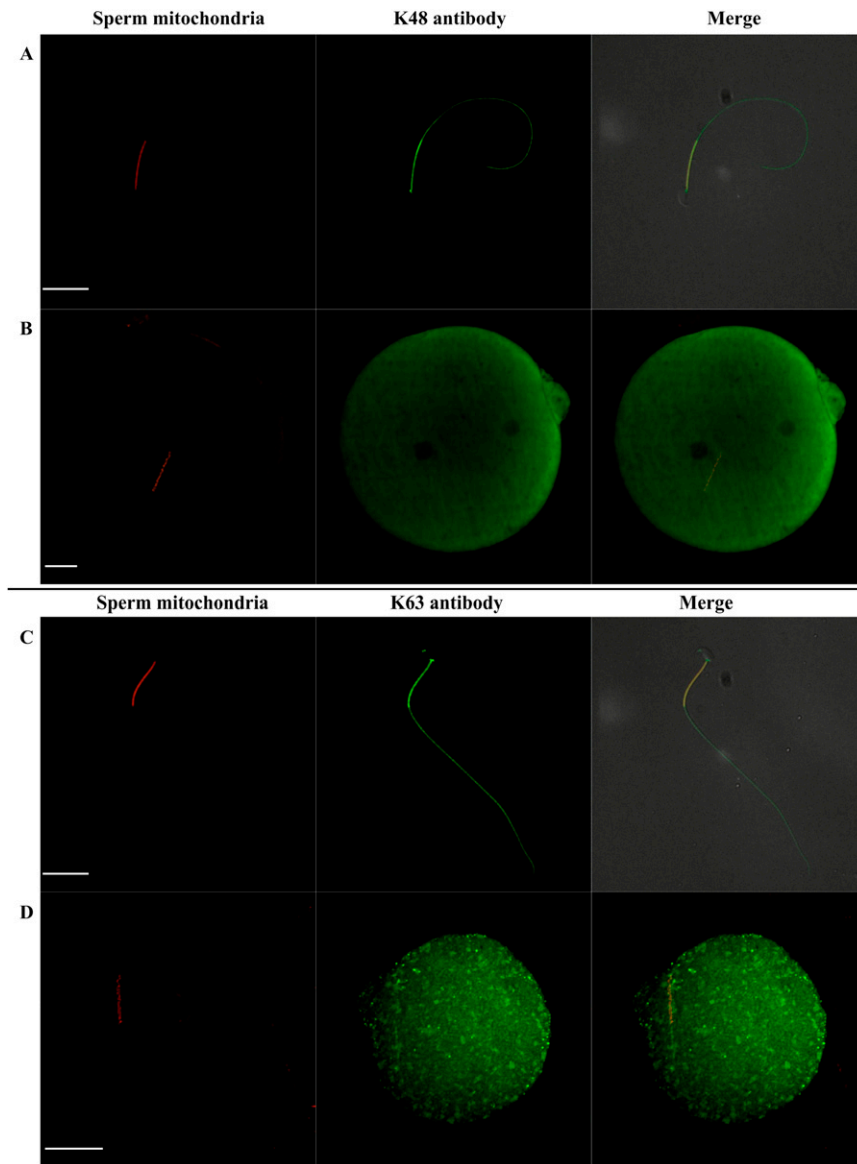


Fig. S2. Immunofluorescence staining of sperm and one-cell-stage embryos with K48 and K63 antibodies (green) as well as sperm mitochondria (red). A and C show entire mouse sperm tail but not mitochondria specifically pre-labeled with K48-linked and K63-linked ubiquitin before fertilization. However, K48-linked ubiquitin was removed at the early pronuclear stage (B), but K63-linked ubiquitin still existed faintly at the one-cell stage (D). (Scale bars: 20 μm .)

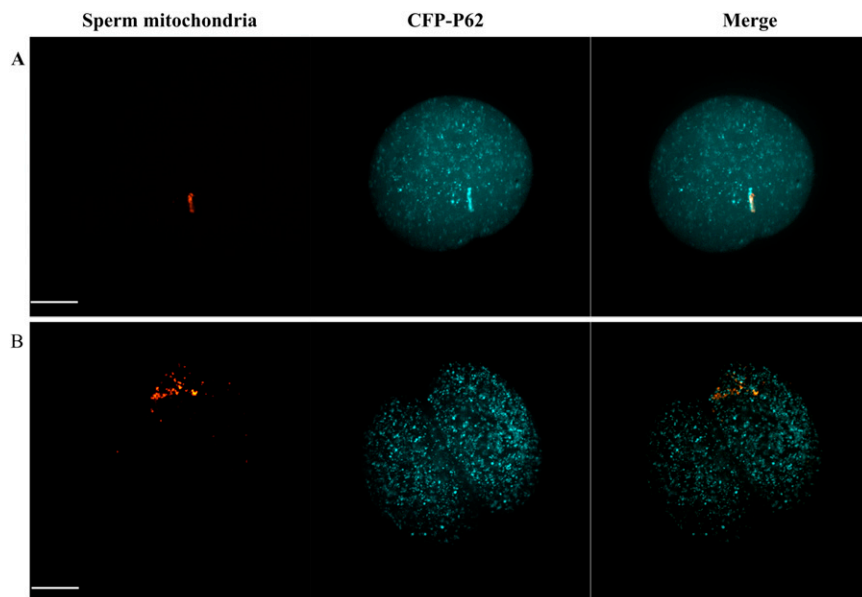


Fig. S3. Live cell fluorescence imaging of sperm mitochondria (red) and CFP-P62 (blue) in early embryos. CFP-P62 was congregated to sperm mitochondria immediately after fertilization (*A*), but became dissociated during the two-cell stage (*B*). (Scale bars: 20 μm .)

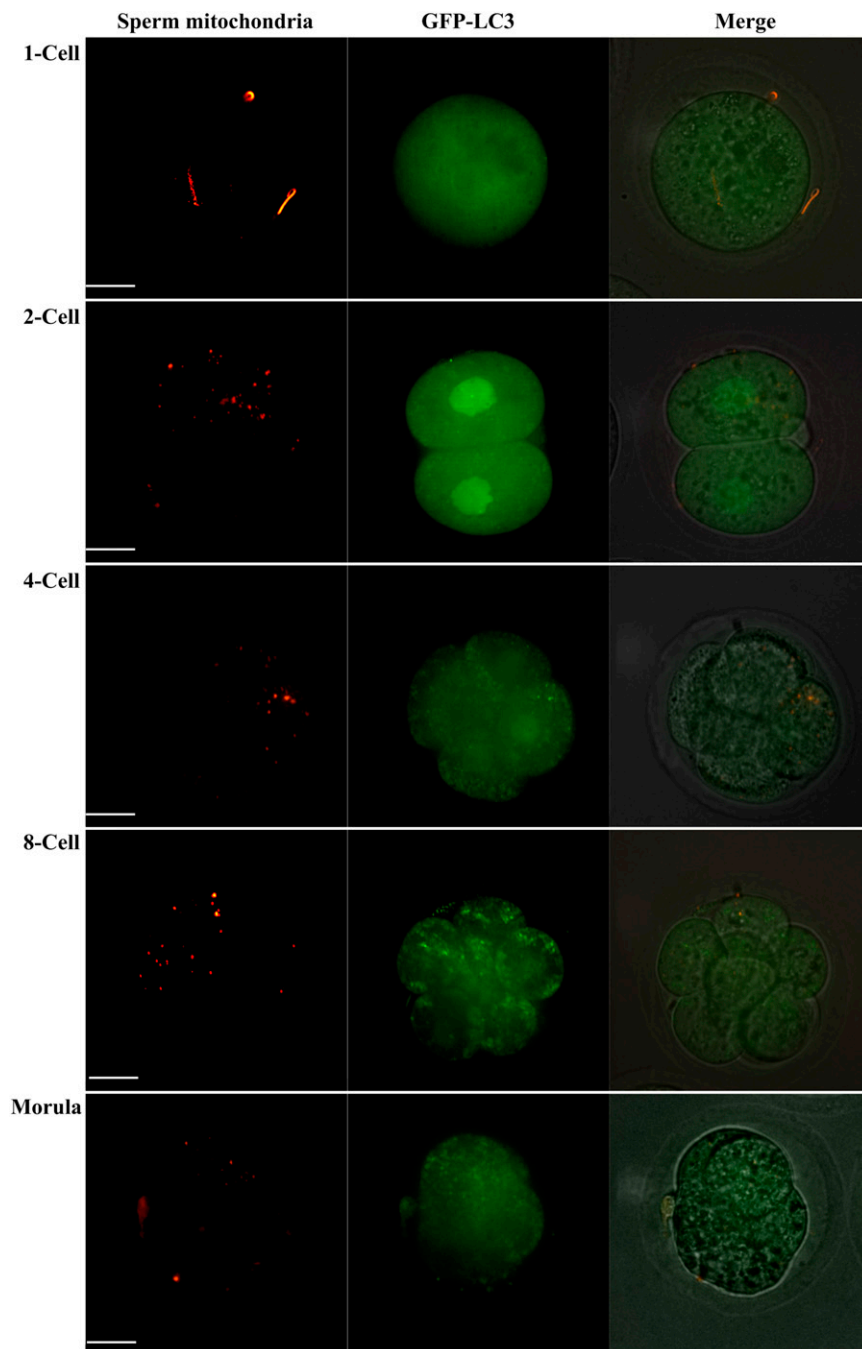


Fig. 54. Live cell fluorescence imaging of sperm mitochondria (red) and GFP-LC3 (green) in *Atg5*-deficient embryos. Autophagy inhibition had no effect on the disaggregation and the fate of sperm mitochondria after fertilization as in Figs. 1 and 2. (Scale bars: 20 μ m.)

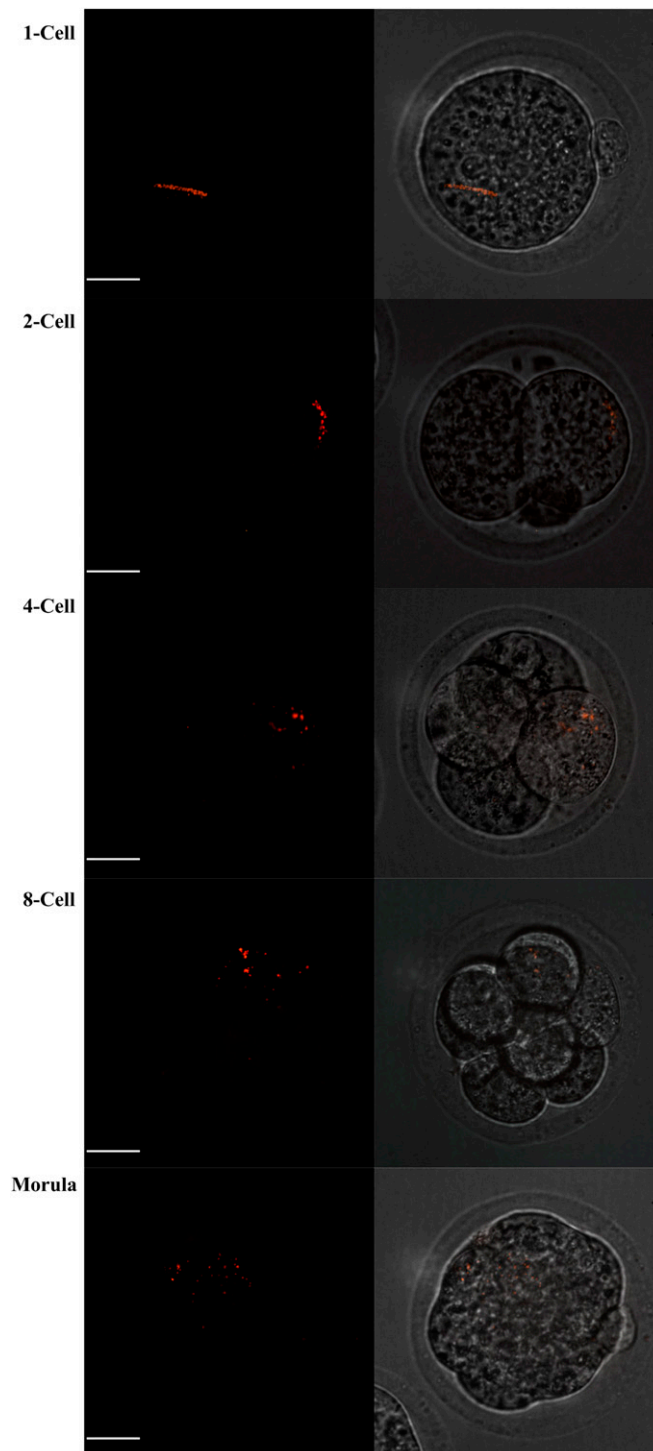


Fig. 55. Live cell fluorescence imaging of sperm mitochondria (red) in sister and brother mating-derived embryos. There was no difference in the dynamic process of the sperm mitochondria between sisters–brothers and BALB/c–C57BL/6j-derived embryos as shown in Fig. 2. (Scale bars: 20 μm .)

```

Balb/c 8941 TAGGAGGCTGCTGACCTCCAACAGGAATTTACCACCTTAACCCCTCTAGAAGTCCCCTACTTAATACTTCAGTACTTCTAGCATCAGGTGTTTCAATTAC
C57/6j 8941 TAGGAGGCTGCTGACCTCCAACAGGAATTTACCACCTTAACCCCTCTAGAAGTCCCCTACTTAATACTTCAGTACTTCTAGCATCAGGTGTTTCAATTAC
9041 ATGAGCTCATCATAGCCTTATAGAAGGTAACGAAACCACATAAATCAAGCCCTACTAATTACCATTATACCTAGGACTTTACTTCACCATCCTCCAAGCT
9141 ATGAGCTCATCATAGCCTTATAGAAGGTAACGAAACCACATAAATCAAGCCCTACTAATTACCATTATACCTAGGACTTTACTTCACCATCCTCCAAGCT
9241 TCAGAATACTTTGAAACATCATTCTCCATTTCCAGATGGTATCTATGGTTCTACATTCTTCATGGCTACTGGATTCCATGGACTCCATGTAATTATTGGAT
9341 CAACATTCCTTATTGTTTGCCTACTACGACAACATAAAATTTCACTTCACATCAAAACATCCTTCCGATTGGAAGCCGAGCATGATACTGACATTTTGT
9441 AGACGTAaTCTGACTTTTCC TATACGTCTCCATTTATTGATGAGGATCTTAC TCCCTTAGTATAAATTAATAAAGTACTGACTTCCAATTAGTAGATTCTGAA
AGACGTAaTCTGACTTTTCC TATACGTCTCCATTTATTGATGAGGATCTTAC TCCCTTAGTATAAATTAATAAAGTACTGACTTCCAATTAGTAGATTCTGAA
9441 TAAACCCAGAAGAGAGTAATcAACCTGTACACTGTTATCTTCATTAATATTTTATTATCCCTAACGCTAATTTCTAGTTGCATTCTGACTCCCCAAATAA
TAAACCCAGAAGAGAGTAATcAACCTGTACACTGTTATCTTCATTAATATTTTATTATCCCTAACGCTAATTTCTAGTTGCATTCTGACTCCCCAAATAA
9541 ATCTGTACTCAGAAAAGCAAAATCCATATGAATGCGGATTCGACCCTACAAGCTCTGCACGCTTACCATTCTCAATAAAATTTTCTTGGTAGCAATTAC
ATCTGTACTCAGAAAAGCAAAATCCATATGAATGCGGATTCGACCCTACAAGCTCTGCACGCTTACCATTCTCAATAAAATTTTCTTGGTAGCAATTAC
9641 ATTTCTATTATTTGACCTAGAAATGCTCTTCTACTTCCACTACCATGAGCAATTCAAACAATTA AACCTCTACTATAATAATATAGCCTTTATCTTA
ATTTCTATTATTTGACCTAGAAATGCTCTTCTACTTCCACTACCATGAGCAATTCAAACAATTA AACCTCTACTATAATAATATAGCCTTTATCTTA
9741 GTCACAATTCATCTCTAGGCCTAGCATATGAATGAACACAAAAGGATTAGAATGAACAGAGTAAATGGTAATTAGTTT. AAAAAAAAAATTAATGATTC
9841 GACTCATTAGATTATGATGATGTTTATAATACCAATATGCCATCTACCTTCTTCAACCT
GACTCATTAGATTATGATGATGTTTATAATACCAATATGCCATCTACCTTCTTCAACCT

```

Fig. S6. Schematic of allele-specific PCR and restriction enzyme identification of paternal (C57/6j) mtDNA. Lowercase indicates different bases between C57/6j and BALB/c mice. Bases underlined are those designed to be sense primer. Bases with double underlining were designed to be antisense primers for allele-specific PCR, which allowed C57/6j mtDNA to be specifically amplified. Bases with dotted underlining allowed C57/6j mouse but not BALB/c mouse mtDNA to be cut with Tth1111 restriction enzyme.

Table S1. Sperm mtDNA distribution in different tissues of newborn mice

Individual no. of F1 hybrids	Endoderm					Mesoderm						Ectoderm Brain	
	Liver	Stomach	Intestine	Pancreas	Lung	Kidney	Spleen	Bladder	Heart	Muscle	Testis		Ovary
Female													
17													+
55													
74				+						+			
83		+										+	
Male													
51			+					+					
63		+								+			
82										+			

Twelve tissues of 93 newborn mice were subjected to examination of paternal mtDNA genome, and plus signs indicate paternal mtDNA existence. Several different tissues were detected to contain paternal mtDNA in seven mice.

Table S2. Detection of mtDNA in single sperm in 45% and 90% density gradient layers and samples not subjected to gradient centrifugation

Mouse	45% layer	90% layer	Sperm not subjected to gradient centrifugation
1	14/24	1/24	10/24
2	15/24	4/24	10/24
3	11/24	3/24	8/24
4	12/24	5/24	9/24
5	10/24	1/24	6/24
Sum	62/120 (51.7)	14/120 (11.7)	43/120 (35.8)

The low rate of sperm mtDNA detected in all three samples indicated that many spermatozoa had eliminated their mtDNA. Values in parentheses are percentages.

Table S3. Primers used for allele-specific PCR and real-time PCR

Primer	Sequence
Allele-specific PCR	
Sense	AGGAATTTCACTTAACC
Antisense 1	GAGTCGAAATCATTATTTTTTCA
Antisense 2	GAAGATAACAGGTACAGGTAA
Preparation of standard samples	
β -Globin sense	GGTTGACTCGCATAGGAA
β -Globin antisense	AAGGAAGAAGCTTGAGGCTTA
Mitochondria sense	AGAGAACTACTAGCCATAGC
Mitochondria antisense	CCACATAGACGAGTTGATTC
Real-time PCR	
β -Globin sense 1	CGAACATACTGAACTGCTA
β -Globin antisense 1	GACATATCTGACATCTCTACTT
Mitochondria sense 1	TACCTCACCATCTCTTGCTA
Mitochondria antisense 1	GCTACACCTTGACCTAACG

For allele-specific PCR, the sense primer was normally designed and was the same one used in the two-cycle PCR, but antisense primer 1 and antisense primer 2 were designed to have mismatched bases at the 3' ends, allowing single copy of paternal (C57/6j) mtDNA specifically amplified even mixed with oocyte (BALB/c) mtDNA.